

of this transition is lower than that for 1. The shoulder around 313 nm is probably the low energy side of the intense charge-transfer ($\pi_L \rightarrow \delta^*$ and π^*) envelope. The other absorptions in the visible region are of very low intensity and may be assigned as the spin-forbidden counterparts of the $\delta \rightarrow \delta^*$ (582 nm) and the LM charge transfer transitions (510 and 479 nm).

The electronic spectrum of $\text{Re}_2(\text{DFM})_4$ has bands at 692, 576, and 367 nm. The band of highest energy is again assigned as the $\delta \rightarrow \delta^*$ transition based on both the calculated MO energies and a comparison with the assignments for 1 and 5. The other two absorptions can be readily assigned as the metal localized dipole allowed $\pi^* \rightarrow \delta^*$ (692 nm) and $\pi^* \rightarrow \sigma^*$ (576 nm) transitions from the calculation.

Concluding Remarks. The molten reaction has been proved to be an effective way to produce $\text{Re}_2(\text{DFM})_4\text{Cl}_2$, and its use is expected to increase in the future to obtain other $\text{Re}_2(\text{LL})_4\text{X}_2$ compounds. On the basis of both the molecular structure and the SCF-X α calculation, a novel $\sigma^2\pi^4\delta^2\pi^*2$ ground state config-

uration has been assigned to $\text{Re}_2(\text{DFM})_4$. Several additional studies of these compounds remain to be pursued. One, obviously, is to be aimed at obtaining the structure of a compound containing the $\text{Re}_2(\text{DFM})_4^+$ ion. Another would be concerned with the magnetic properties, including EPR spectra, of the $\text{Re}_2(\text{DFM})_4^+$ and $\text{Re}_2(\text{DFM})_4$ species. Preliminary EPR results are already in hand, but we cannot yet interpret them. New computer simulation programs are necessary to deal with these dinuclear systems.

Acknowledgment. We thank the National Science Foundation for support.

Supplementary Material Available: Complete tables of crystal data, bond distances and angles, and anisotropic displacement parameters for structures 1, 3, 4, and 5 and tables of valence molecular orbitals for A, B, and C (43 pages); tables of observed and calculated structure factors (67 pages). Ordering information is given on any current masthead page.

A Face-Capping Bonding Mode for Benzene in Triosmium Carbonyl Cluster Complexes

Mark A. Gallop, M. Pilar Gomez-Sal, Catherine E. Housecroft,* Brian F. G. Johnson, Jack Lewis,* Steven M. Owen, Paul R. Raithby,* and Anthony H. Wright¹

Contribution from the University Chemical Laboratory, Lensfield Road, Cambridge, CB2 1EW, U.K. Received October 11, 1989. Revised Manuscript Received October 23, 1991

Abstract: This paper describes the synthesis of trinuclear metal complexes containing benzene in a new face-capping bonding mode, $(\mu_3:\eta^2:\eta^2:\eta^2\text{-C}_6\text{H}_6)$, that accurately models the coordination geometry of benzene chemisorbed nondissociatively on the surface of a close-packed metal lattice. $[\text{Os}_3(\text{CO})_9(\mu_3:\eta^2:\eta^2:\eta^2\text{-C}_6\text{H}_6)]$ (1), the parent complex, is elaborated through stepwise "dehydrogenation" of the triply-bridging cyclohexadienyl compound $[(\mu\text{-H})\text{Os}_3(\text{CO})_9(\mu_3:\eta^2:\eta^2:\eta^2\text{-C}_6\text{H}_7)]$, and an X-ray diffraction analysis reveals intriguing multiple bond fixation within the coordinated arene: Im , $a = 8.412$ (1) Å, $b = 35.449$ (4) Å, $c = 8.877$ (1) Å, $\beta = 92.44$ (1)°, $V = 2644.7$ Å³, $Z = 6$, $R = 3.2\%$, $R_w = 3.4\%$ for 2465 reflections with $F_o > 4\sigma(F_o)$. The ring symmetrically caps a trimetal face and shows Kekulé-type distortion toward the hypothetical cyclohexa-1,3,5-triene (on average, C-C bond lengths alternate between 1.41 (3) and 1.51 (4) Å). The preparation of an analogous toluene complex, $[\text{Os}_3(\text{CO})_9(\mu_3:\eta^2:\eta^2:\eta^2\text{-C}_6\text{H}_5\text{Me})]$ is also reported. Oxidative decarbonylation of 1 by trimethylamine *N*-oxide in the presence of MeCN affords the lightly-ligated complex $[\text{Os}_3(\text{CO})_8(\text{NCMe})(\mu_3:\eta^2:\eta^2:\eta^2\text{-C}_6\text{H}_6)]$ (9). Two-electron donor ligands (e.g., CO, PR₃, C₃H₅N, olefins) readily displace the labile nitrile ligand from 9, giving derivatives $[\text{Os}_3(\text{CO})_8(\text{L})(\mu_3:\eta^2:\eta^2:\eta^2\text{-C}_6\text{H}_6)]$ that retain the face-capping benzene moiety. The molecular structures of $[\text{Os}_3(\text{CO})_8(\text{PPh}_3)(\mu_3:\eta^2:\eta^2:\eta^2\text{-C}_6\text{H}_6)]$ and $[\text{Os}_3(\text{CO})_8(\eta^2\text{-CH}_2\text{CH}_2)(\mu_3:\eta^2:\eta^2:\eta^2\text{-C}_6\text{H}_6)]$ have been determined by X-ray crystallography and are derived from that of complex 1, with an equatorial carbonyl ligand being replaced by triphenylphosphine and a π -bound ethylene ligand, respectively. The cluster $[\text{Os}_3(\text{CO})_8(\text{PPh}_3)(\mu_3:\eta^2:\eta^2:\eta^2\text{-C}_6\text{H}_6)]$ crystallizes in space group $P2_1/c$ with $a = 13.381$ (5) Å, $b = 14.894$ (5) Å, $c = 16.896$ (7) Å, $\beta = 113.33$ (3)°, $V = 3092.0$ Å³, $Z = 4$, $R = 3.9\%$, $R_w = 4.1\%$ for 4747 reflections with $F_o > 4\sigma(F_o)$. The cluster $[\text{Os}_3(\text{CO})_8(\eta^2\text{-CH}_2\text{CH}_2)(\mu_3:\eta^2:\eta^2:\eta^2\text{-C}_6\text{H}_6)]$ crystallizes in space group $P2_1/n$ with $a = 8.876$ (1) Å, $b = 14.665$ (2) Å, $c = 14.178$ (2) Å, $\beta = 92.56$ (2)°, $V = 1843.7$ Å³, $Z = 4$, $R = 4.8\%$, $R_w = 4.8\%$ for 1890 reflections with $F_o > 4\sigma(F_o)$. Semiempirical molecular orbital calculations provide useful insights into the structure and bonding of complex 1. Primary contributions to metal-arene bonding arise from overlap of the benzene HOMO with the LUMO of the cluster fragment and through π -back donation to the benzene LUMO from a high-lying cluster-based molecular orbital. The trigonal ring distortion may be traced to an internal mixing of the benzene π system that leads to increased overlap in the C-C bonds eclipsing the metal atoms, at the expense of the alternate noneclipsing bonds which consequently become elongated. Possible relationships between these compounds and aromatic adsorbate complexes of transition metal surfaces are also explored.

Arene coordination chemistry is truly diverse.² η^6 -Ligation is virtually ubiquitous amongst the transition metals, and η^6 -arene ligands have been structurally characterized in a variety of polynuclear metal complexes.³ Formal donation of six electrons

from these cyclic π -systems is not mandatory, however, and arenes may behave as pseudo-diene⁴ or olefinic⁵ ligands in η^4 - and η^2 -

(1) Present address: Department of Chemistry, The University, Nottingham, NG7 2RD, U.K.

(2) (a) Zeiss, H.; Wheatley, P. J.; Winkler, H. J. *S. Benzenoid-Metal Complexes*; Ronald Press Co.: New York, 1966. (b) Silverthorn, W. E. *Adv. Organomet. Chem.* 1975, 13, 47. (c) Gasting, R. G.; Klabunde, K. J. *Transition Met. Chem.* 1979, 4, 1. (d) Muetterties, E. L.; Bleck, J. R.; Wucherer, E. J.; Albright, T. A. *Chem. Rev.* 1982, 82, 499.

(3) (a) Dellaca, R. J.; Penfold, B. R. *Inorg. Chem.* 1972, 11, 1855. (b) Churchill, M. R.; Chang, S. W.-Y. *J. Chem. Soc., Chem. Commun.* 1974, 248. (c) Goldberg, S. Z.; Spivack, B.; Stanley, G.; Eisenberg, R.; Braitsch, D. M.; Miller, J. S.; Abkowitz, M. *J. Am. Chem. Soc.* 1977, 99, 110. (d) Aime, S.; Milone, L.; Osella, D.; Vaglio, G. A.; Valle, M.; Tiripicchio, A.; Tiripicchio Camellini, M. *Inorg. Chim. Acta* 1979, 34, 49. (e) Bird, P. H.; Fraser, A. R. *J. Organomet. Chem.* 1974, 73, 103. (f) Garcia, M. P.; Green, M.; Stone, F. G. A.; Sommerville, R. G.; Welch, A. J. *J. Chem. Soc., Chem. Commun.* 1981, 871. (g) Gould, R. O.; Jones, C. L.; Robertson, D. R.; Tocher, D. A.; Stephenson, T. A. *J. Organomet. Chem.* 1982, 226, 199.

coordination modes, respectively. In these compounds the arene ring parameters may diverge substantially from those of the free ligands; ring planarity is lost, and there is extensive localization of single and double bonds in the uncomplexed fragment. An early hypothesis⁶ that η^2 -complexes may be important intermediates in arene activation reactions has recently been verified independently by Graham⁷ and Jones.⁸ Arenes can also act as bridging ligands between two metal atoms. This bridge-bonding may occur either syn-facially⁹ or anti-facially^{5a} with respect to the C_6 ring, or both, as in the triple-decker sandwich compound $[\{V(\eta^5-C_5H_5)\}_2(\mu:\eta^6:\eta^6-C_6H_6)]$, where a planar benzene ligand forms the middle deck of the complex.¹⁰

In 1985 we reported a new coordination mode for benzene in the carbonyl cluster complexes $[Os_3(CO)_9(\mu_3:\eta^2:\eta^2:\eta^2-C_6H_6)]$ (1) and $[Ru_6C(CO)_{11}(\eta^6-C_6H_6)(\mu_3:\eta^2:\eta^2:\eta^2-C_6H_6)]$ (2) where the ring is symmetrically bonded over the face of a metal triangle.¹¹ The carbido cluster 2 is isolated as the major product from the reaction of $[Ru_6C(CO)_{13}(\eta^6-C_6H_6)]^{2-}$ with $[Ru(\eta^6-C_6H_6)(NCPH)_3]^{2+}$; any heptanuclear intermediate formed must be very labile with respect to cluster decapping, and the benzene transition from η^6 -terminal to $\mu_3:\eta^2:\eta^2:\eta^2$ -face-capping occurs during the course of the reaction.

The structure of 2 is derived from the parent hexaruthenium carbido carbonyl $[Ru_6C(CO)_{17}]$ ¹² by substitution of a conventionally η^6 -coordinated benzene for three terminal CO ligands at an apical ruthenium atom and replacement of three carbonyls at a triruthenium face by the capping ($\mu_3:\eta^2:\eta^2:\eta^2-C_6H_6$) ligand. The two CO ligands at each Ru atom of the capped face are almost coplanar with the metal triangle, and the plane of the benzene ring makes an angle of 0.5° with the Ru_3 plane. An intriguing feature of the structure is the alternation of bond lengths around the C_6 ring. The lengths of the C-C bonds that span the Ru atoms average 1.39 (2) Å, while the unattached C-C bond lengths average 1.48 (2) Å. In the nomenclature of valence-bond theory, the apparent bond localization in the face-capping benzene represents a Kekule-type distortion of the ring toward the hypothetical cyclohexatriene, coordinated as a triolefin via its three double bonds to the ruthenium atoms of a triangular face. The triosmium complex (1) features the same μ_3 -coordination mode for benzene, and in this paper the synthesis, structure, bonding, and ligand substitution chemistry of this compound are described in detail. Interest in these novel complexes is heightened by the realization

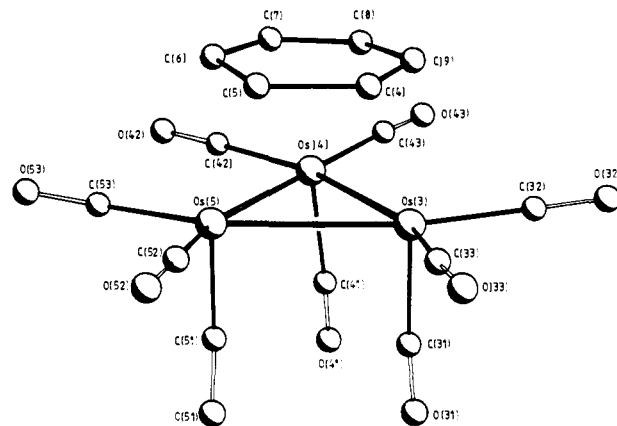
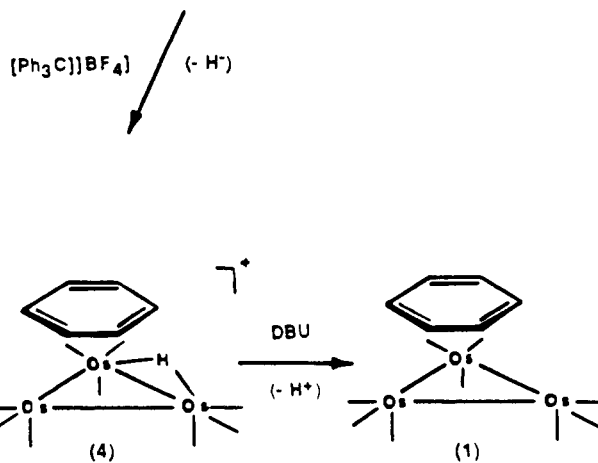
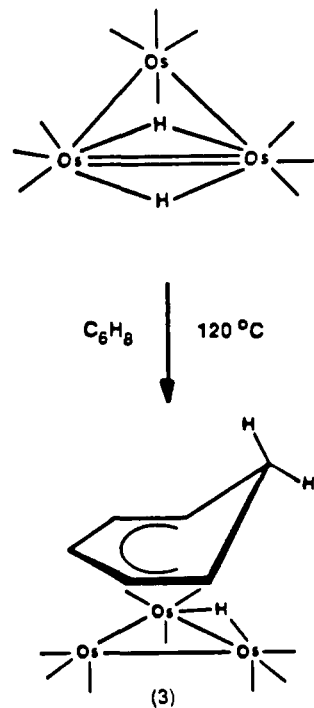


Figure 1. Molecular structure of $[Os_3(CO)_9(\mu_3:\eta^2:\eta^2:\eta^2-C_6H_6)]$ (1).

Scheme I. Synthesis of $[Os_3(CO)_9(\mu_3:\eta^2:\eta^2:\eta^2-C_6H_6)]$ (1)



that the ($\mu_3:\eta^2:\eta^2:\eta^2-C_6H_6$) ligands bear a striking resemblance to benzene chemisorbed at 3-fold sites in CO-coadsorbate overlayers on the close-packed Rh(111) surface.¹³ The proposition

(4) (a) Bandy, J. A.; Green, M. L. H.; O'Hare, D.; Prout, K. *J. Chem. Soc., Chem. Commun.* **1984**, 1402. (b) Boncella, J. M.; Green, M. L. H.; O'Hare, D. *J. Chem. Soc., Chem. Commun.* **1986**, 618. (c) Boncella, J. M.; Green, M. L. H. *J. Organomet. Chem.* **1987**, 325, 217. (d) Huttner, G.; Lange, S. *Acta Crystallogr.* **1972**, B28, 2049. (e) Churchill, M. R.; Mason, R. *Proc. R. Soc. London, Ser. A* **1966**, 292, 61. (f) Lucherini, A.; Porri, L. *J. Organomet. Chem.* **1978**, 155, C45. (g) Barlex, D. M.; Evans, J. A.; Kemmitt, R. D. W.; Russell, D. R. *J. Chem. Soc., Chem. Commun.* **1971**, 331. (h) Bond, A.; Bottrill, M.; Green, M.; Welch, A. J. *J. Chem. Soc., Dalton Trans.* **1977**, 2372.

(5) (a) van der Heijden, H.; Orpen, A. G.; Pasman, P. *J. Chem. Soc., Chem. Commun.* **1985**, 1576. (b) Harman, W. D.; Taube, H. *J. Am. Chem. Soc.* **1987**, 109, 1883. (c) Browning, J.; Green, M.; Penfold, B. R.; Spencer, J. L.; Stone, F. G. A. *J. Chem. Soc., Chem. Commun.* **1973**, 31. (d) Cobble, R. E.; Einstein, F. W. B. *Acta Crystallogr.* **1978**, B34, 1849. (e) Brauer, D. J.; Kruger, C. *Inorg. Chem.* **1977**, 16, 884. (f) Klein, H.-F.; Ellrich, K.; Lamac, S.; Lull, G.; Zsolnai, L.; Huttner, G. *Z. Naturforsch.* **1985**, 40B, 1377. (g) Hall Griffith, E. A.; Amma, E. L. *J. Am. Chem. Soc.* **1974**, 96, 5407 and references therein. (h) Uson, R.; Laguna, A.; Laguna, M.; Manzano, B. R.; Jones, P. G.; Sheldrick, G. M. *J. Chem. Soc., Dalton Trans.* **1984**, 285. (i) There is a unique example of η^1 -benzene coordination in the compound $[Ag(\eta^1-C_6H_6)(B_{10}CH_{12})-(C_6H_6)]$, see: Shelly, K.; Finster, D. C.; Lee, Y. J.; Scheidt, W. R.; Reed, C. A. *J. Am. Chem. Soc.* **1985**, 107, 5955.

(6) (a) Chatt, J.; Davidson, J. M. *J. Chem. Soc.* **1965**, 843. (b) Parshall, G. W. *Homogeneous Catalysis*; John Wiley and Sons: New York, 1980.

(7) Sweet, J. R.; Graham, W. A. G. *Organometallics* **1983**, 2, 135.

(8) Jones, W. D.; Feher, F. J. *J. Am. Chem. Soc.* **1984**, 106, 1650.

(9) (a) Allegra, G.; Tettamanti Casagrande, G.; Immirzi, A.; Porri, L.; Vitulli, G. *J. Am. Chem. Soc.* **1970**, 92, 289. (b) Nardin, G.; Delise, P.; Allegra, G. *Gazz. Chim. Ital.* **1975**, 105, 1047. (c) Jonas, K.; Wiskamp, V.; Tsay, Y.-H.; Kruger, C. *J. Am. Chem. Soc.* **1983**, 105, 5480.

(10) Duff, A. W.; Jonas, K.; Goddard, R.; Kraus, H.-J.; Kruger, C. *J. Am. Chem. Soc.* **1983**, 105, 5479.

(11) Gomez-Sal, M. P.; Johnson, B. F. G.; Lewis, J.; Raithby, P. R.; Wright, A. H. *J. Chem. Soc., Chem. Commun.* **1985**, 1682.

(12) Mason, R.; Robinson, W. R. *J. Chem. Soc., Chem. Commun.* **1968**, 468.

Table I. Crystallographic Data for $[\text{Os}_3(\text{CO})_9(\mu_3\eta^2\text{-}\eta^2\text{-}\eta^2\text{-C}_6\text{H}_6)]$ (**1**), $[\text{Os}_3(\text{CO})_8(\text{PPh}_3)(\mu_3\eta^2\text{-}\eta^2\text{-}\eta^2\text{-C}_6\text{H}_6)]$ (**10**), and $[\text{Os}_3(\text{CO})_8(\eta^2\text{-CH}_2\text{CH}_2)(\mu_3\eta^2\text{-}\eta^2\text{-}\eta^2\text{-C}_6\text{H}_6)]$ (**11**)

	1	10	11
(a) Crystal Parameters			
formula	$\text{C}_{15}\text{H}_6\text{O}_9\text{Os}_3$	$\text{C}_{32}\text{H}_{21}\text{O}_8\text{P}\text{Os}_3$	$\text{C}_{16}\text{H}_{10}\text{O}_8\text{Os}_3$
mol wt	900.84	1135.06	900.84
crystal system	monoclinic	monoclinic	monoclinic
space group	<i>Im</i>	$P2_1/c$	$P2_1/n$
<i>a</i> , Å	8.412 (1)	13.381 (5)	8.876 (1)
<i>b</i> , Å	35.449 (4)	14.894 (5)	14.665 (2)
<i>c</i> , Å	8.877 (1)	16.896 (7)	14.178 (2)
β , deg	92.44 (1)	113.33 (3)	92.56 (2)
<i>V</i> , Å ³	2644.7	3092.0	1843.7
temp (+2 °C)	17	16	16
<i>Z</i>	6	4	4
μ , cm ⁻¹	216.07	123.79	206.59
ρ , g cm ⁻³ (calcd)	3.39	2.44	3.24
size, mm	0.12 × 0.21 × 0.34	0.22 × 0.27 × 0.30	0.07 × 0.12 × 0.12
(b) Data Collection			
radiation	Mo K α	Mo K α	Mo K α
λ , Å	0.71069	0.71069	0.71069
monochromator	graphite	graphite	graphite
2 θ scan range, deg	5–50	5–50	5–45
scan type	ω	ω	ω/θ
ω scan width, deg	0.96	0.96	1.44
std reflns	3 h ⁻¹	3 h ⁻¹	3 h ⁻¹
(c) Data Reduction and Refinement			
reflens collected	4964	11913	2720
unique reflens	2527	5428	2414
unique reflens with $F_o > n\sigma(F_o)$	2465 (<i>n</i> = 4)	4747 (<i>n</i> = 4)	1890 (<i>n</i> = 4)
absorption correction	applied	applied	applied
transmission coeff			
max.	0.071	0.127	0.121
min.	0.014	0.015	0.022
$R_F\%$	3.2	3.9	4.8
$R_w\%$ (<i>g</i> value)	3.4 (0.0004)	4.1 (0.0005)	4.8 (0.001)
highest peak, final diff Fourier, eÅ ⁻³	1.80	1.75	1.83
largest shift/error			
value of final cycle	0.02	0.04	0.06

that discrete molecular compounds may be reasonable models of metal surfaces in the processes of chemisorption and catalysis has recently provoked considerable speculation,¹⁴ and we believe that studies in this cluster system may provide fresh insight into the surface chemistry of benzene and other aromatic species, while concurrently highlighting possible boundary conditions to any analogy between clusters and surfaces.

Results and Discussion

Synthesis and Structure of $[\text{Os}_3(\text{CO})_9(\mu_3\eta^2\text{-}\eta^2\text{-}\eta^2\text{-C}_6\text{H}_6)]$ (1**).** In the synthetic approach to the triosmium complex $[\text{Os}_3(\text{CO})_9(\mu_3\eta^2\text{-}\eta^2\text{-}\eta^2\text{-C}_6\text{H}_6)]$ (**1**), the face-capping ligand is elaborated through stepwise "dehydrogenation" of a triply-bridging cyclohexadienyl complex $[(\mu\text{-H})\text{Os}_3(\text{CO})_9(\mu_3\eta^2\text{-}\eta^1\text{-}\eta^2\text{-C}_6\text{H}_7)]$ (**3**), formed by reaction of $[(\mu\text{-H})_2\text{Os}_3(\text{CO})_{10}]$ with 1,3- or 1,4-cyclohexadiene.¹⁵ The triphenylmethyl (trityl) cation abstracts hydride from the dienyl ring in **3** to generate the cationic hydrido-benzene complex $[(\mu\text{-H})\text{Os}_3(\text{CO})_9(\mu_3\eta^2\text{-}\eta^2\text{-}\eta^2\text{-C}_6\text{H}_6)]^+$ (**4**), which is readily deprotonated at the metal triangle by the non-nucleophilic base DBU, affording the μ_3 -benzene cluster **1** in good

yield. This chemistry is summarized in Scheme I.

The nature of complex **1** has been confirmed by a single-crystal X-ray diffraction study. Compound **1** crystallizes in the monoclinic space group *Im*, a nonstandard setting of *Cm*, with 1.5 molecules per asymmetric unit, a crystallographic mirror plane passing through one molecule. There are no close intermolecular contacts. The structure of the crystallographically independent molecule is illustrated in Figure 1, with selected structural parameters presented in Table I and Tables S2A and S3A (supplementary material). The benzene-capped triosmium cluster (**1**) has approximate C_{3v} symmetry, and the metal-metal distances are comparable to those found in $[\text{Os}_3(\text{CO})_{12}]$ (av Os–Os = 2.877 (3) Å).¹⁶ The plane of the C_6H_6 ring makes an angle of only 1.1° with the plane defined by the Os atoms and the equatorial carbonyl ligands, indicating that the two units are essentially parallel. The pattern of alternating "long" and "short" bond lengths observed in the hexaruthenium complex (**2**)¹¹ is again suggested for the ring in **1** (mean "coordinated" and "noncoordinated" C–C distances are 1.41 (3) and 1.51 (4) Å, respectively) although the high estimated standard deviations associated with these distances renders this variation statistically insignificant at the 2 σ level.

Face-capping coordination has very recently been established for *trans*- β -methylstyrene in the cobalt cluster complex $[(\text{CpCo})_3(\mu_3\eta^2\text{-}\eta^2\text{-}\eta^2\text{-C}_6\text{H}_5\text{CH}=\text{CHMe})]$ (**5**) through an X-ray structure analysis of high precision.¹⁷ In marked contrast to carbonyl clusters **1** and **2** the C–C bond lengths in the aromatic ring here show almost negligible alternation (mean distances 1.420

(13) (a) Lin, R. F.; Blackman, G. S.; Van Hove, M. A.; Somorjai, G. A. *Acta Crystallogr.* **1987**, *B43*, 368. (b) Van Hove, M. A.; Lin, R. F.; Somorjai, G. A. *J. Am. Chem. Soc.* **1986**, *108*, 2532.

(14) (a) Muettterties, E. L. *Bull. Soc. Chim. Belg.* **1975**, *84*, 959. (b) Muettterties, E. L. *Science* **1977**, *196*, 839. (c) Muettterties, E. L. *Pure Applied Chem.* **1978**, *50*, 941. (d) Muettterties, E. L. *Angew. Chem., Int. Ed. Engl.* **1978**, *17*, 545. (e) Muettterties, E. L.; Rhodin, T. N.; Band, E.; Brucker, C. F.; Pretzer, W. *Chem. Rev.* **1979**, *79*, 91. (f) Muettterties, E. L. *Pure and Appl. Chem.* **1982**, *54*, 83. (g) Moskovits, M. *Acc. Chem. Res.* **1979**, *12*, 229. (h) Evans, J. *Chem. Soc. Rev.* **1981**, *10*, 159. (i) Ertl, G. In *Metal Clusters in Catalysis*; Gates, B. C., Gucci, L., Knozinger, H., Eds.; Elsevier: Amsterdam, 1986. (j) Basset, J. M.; Choplin, A. *J. Mol. Catal.* **1983**, *21*, 95.

(15) Bryan, E. G.; Johnson, B. F. G.; Kelland, J. W.; Lewis, J.; McPartlin, M. *J. Chem. Soc., Chem. Commun.* **1976**, 254.

(16) Churchill, M. R.; de Boer, B. G. *Inorg. Chem.* **1977**, *16*, 878.

(17) Wadephol, H.; Buchner, K.; Pritzkow, H. *Angew. Chem., Int. Ed. Engl.* **1987**, *26*, 1259.

(5) and 1.446 (5) Å) illustrating that pronounced Kekulé distortion of an arene is not an intrinsic property of its coordination at a 3-fold metal site. We shall see that benzene bond fixation in the triosmium system is a sensitive function of the supporting ligand sphere and suggest through Fenske–Hall molecular orbital calculations an electronic basis for this alternation. The ring substituents are displaced away from the metal triangle in **5** by some 10–18°, and a comparable distortion is anticipated in complex **1** where the benzene protons have not been accurately located. Spectroscopic and theoretical studies presented below are also consistent with C–H bond back-bending in **1**.

Spectroscopy of the $\mu_3:\eta^2:\eta^2:\eta^2\text{-C}_6\text{H}_6$ Ligand. Infrared spectroscopic studies indicate that $\nu_{\text{C-H}}$ modes for the terminal and face-capping arene ligands occur at significantly different energies. Vibrational modes of a_1/e symmetry for μ_1 - and μ_3 -benzene are seen at, respectively, 3125/3118 and 3100/3065 cm^{-1} in **2** and at 3104/3071 cm^{-1} in **1**. This suggests that the transition from η^6 -apical to face-capping coordination is accompanied by partial rehybridization ($sp^2 \rightarrow sp^3$) of the ring carbons (i.e., an out-of-plane distortion of the C–H bonds), a consequence, perhaps, of increase π -acceptance from the cluster in the triply bridging mode. The frequency of the symmetric metal-ring stretch (326 cm^{-1} in **1**) falls by some 30 cm^{-1} on protonation, indicating a weaker benzene–cluster interaction in the cation **4**. We interpret this effect as reflecting a decrease in metal-to-arene π -back bonding arising from the stabilization of the π -donor orbitals of the cluster fragment. The importance of this π -interaction is reiterated in our MO description of the metal–ligand bonding (vide infra).

The η^6 -terminal and $\mu_3:\eta^2:\eta^2:\eta^2$ -capping modes for benzene may be readily distinguished by NMR spectroscopy, with resonances for the μ_3 -ligand being found to substantially higher field in both the ^1H and ^{13}C NMR spectra. Thus, a singlet resonance at δ 4.42 in the ^1H spectrum of **1** should be compared with a typical chemical shift for the η^6 -ligand of δ 5.07 in $[\text{Os}(\text{P}(\text{OMe})_3)_2(\eta^6\text{-C}_6\text{H}_6)]$,¹⁸ while in **2** singlets at δ 5.54 and δ 4.14 may be assigned to the proton resonances of the apical and face-capping benzene ligands, respectively. In the $^{13}\text{C}\{^1\text{H}\}$ NMR spectrum of **1** a single resonance is observed for the ring carbons at δ 38.15, representing an upfield shift of ca. 90 ppm from the uncomplexed arene. Coordination shifts in the ^{13}C spectra of mononuclear chromium benzene complexes have been noted previously,¹⁹ though the shieldings are significantly smaller for the $\eta^6\text{-C}_6\text{H}_6$ ligand. The source of these high field shifts remains poorly understood but has been discussed in terms of metal–ligand bond anisotropy, modification of ring current contributions, changes in hybridization at the ring carbon atoms, or electron density changes.¹⁹ The ^{13}C shift is a sum of local and nonlocal contributions of a diamagnetic shielding term as well as a paramagnetic shielding term,²⁰ and calculations by Brown et al. support the suggestion that trends in carbon atom chemical shifts in transition metal organometallic systems can be analyzed through changes in the paramagnetic term σ^p .²¹ While increased shielding in the benzene cluster complexes would appear consistent with greater π -acidity for the μ_3 -ligand,²² a qualitative interpretation of ^{13}C shifts is hampered by the fact that σ^p is dependent on three terms in the Pople–Karplus expression²³ that may be separately influenced by σ - and π -bonding effects.

Substitution Chemistry of $[\text{Os}_3(\text{CO})_9(\mu_3:\eta^2:\eta^2:\eta^2\text{-C}_6\text{H}_6)]$: Synthesis and Reactivity of $[\text{Os}_3(\text{CO})_8(\text{NCMe})(\mu_3:\eta^2:\eta^2:\eta^2\text{-C}_6\text{H}_6)]$. The formal triene-like representation of the face-capping ligand in $[\text{Os}_3(\text{CO})_9(\mu_3:\eta^2:\eta^2:\eta^2\text{-C}_6\text{H}_6)]$ (**1**) belies the remarkable robustness

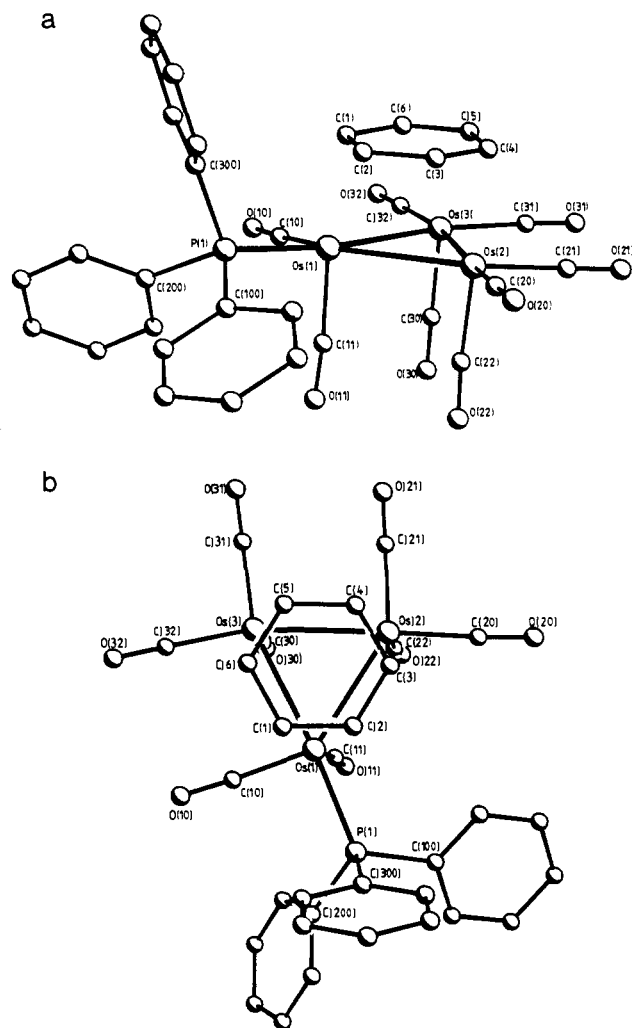


Figure 2. Molecular structure of $[\text{Os}_3(\text{CO})_8(\text{PPh}_3)(\mu_3:\eta^2:\eta^2:\eta^2\text{-C}_6\text{H}_6)]$ (**10**).

of this complex, and harsh reaction conditions are typically required for arene displacement. The carbonyl substitution chemistry of **1** resembles that of the parent dodecacarbonyl $[\text{Os}_3(\text{CO})_{12}]$ (**6**),²⁴ with its thermally-promoted reactions proceeding rather inefficiently and with low selectivity. Oxidative decarbonylation by trimethylamine *N*-oxide has been used extensively in the activation of the latter complex toward CO substitution; nucleophilic activation in the presence of the weak-field ligand MeCN affords the labile derivatives $[\text{Os}_3(\text{CO})_{12-n}(\text{NCMe})_n]$ [$n = 1$ (**7**), 2 (**8**)] that are versatile starting materials for the synthesis of many triosmium cluster compounds.^{25,32} This strategy has been successfully applied to the derivatization of **1**, reaction with an equimolar quantity of anhydrous Me_3NO in acetonitrile affords in high yield the deep yellow complex $[\text{Os}_3(\text{CO})_8(\text{NCMe})(\mu_3:\eta^2:\eta^2:\eta^2\text{-C}_6\text{H}_6)]$ (**9**) as two isomers.

^1H NMR spectroscopy confirms the formulation of this product and indicates high lability for the nitrile ligand: at 295 K, in CD_3CN solution a broad singlet resonance at δ 4.34 is assigned to the fluxional μ_3 -benzene ligand, while a singlet at δ 1.97 is attributed to free MeCN, displaced from the cluster by exchange with the solvent. On recording the spectrum of a solution of **9** prepared at 195 K in the mixed solvent system $\text{CD}_2\text{Cl}_2/\text{CD}_3\text{CN}$ (10:1), three broadened singlets (δ 4.06, 3.94, and 3.68) attributed to the ring protons of the minor, equatorially substituted isomer (**9b**) are observed in addition to the single broad resonance (δ 4.4) of the major axially substituted isomer (**9a**) (integrated intensities

(18) Werner, H.; Werner, R. *J. Organomet. Chem.* **1980**, *194*, C7.
 (19) (a) Thoenes, D. J.; Wilkins, C. L.; Trahanovsky, W. S. *J. Magn. Reson.* **1974**, *13*, 18 and references therein. (b) Graves, V.; Lagowski, J. J. *J. Organomet. Chem.* **1976**, *120*, 397. (c) Farnell, L. F.; Randall, E. W.; Rosenberg, E. *J. Chem. Soc., Chem. Commun.* **1971**, 1078. (d) Langer, E.; Lehner, H. *J. Organomet. Chem.* **1979**, *173*, 47.
 (20) Saika, A.; Slichter, C. P. *J. Chem. Phys.* **1954**, *22*, 26.
 (21) Brown, D. A.; Chester, J. P.; Fitzpatrick, N. J.; King, I. J. *Inorg. Chem.* **1977**, *16*, 2497.
 (22) Mann, B. E.; Taylor, B. F. *^{13}C NMR Data for Organometallic Compounds*; Academic Press: London, 1981.
 (23) Karplus, M.; Pople, J. A. *J. Chem. Phys.* **1963**, *38*, 2803.

(24) (a) Johnson, B. F. G.; Lewis, J. *Adv. Inorg. Radiochem.* **1981**, *24*, 225. (b) Deeming, A. J. *Adv. Organomet. Chem.* **1986**, *26*, 1.
 (25) Tachikawa, M.; Shapley, J. R. *J. Organomet. Chem.* **1977**, *124*, C19.

1:5). Resonances at δ 2.80 and δ 2.33 for the minor and major isomers, respectively, rapidly lose intensity on warming to room temperature, being replaced by a sharp singlet at δ 1.97, consistent with facile displacement of coordinated MeCN by the deuterated solvent.

Substitution by Phosphorus Donor Ligands. Phosphine substitution for CO in $[\text{Os}_3(\text{CO})_{12}]$ (**6**) invariably occurs at an equatorial site^{24b} and a single-crystal X-ray diffraction study reveals equatorial coordination of triphenylphosphine in the μ_3 -benzene complex $[\text{Os}_3(\text{CO})_8(\text{PPh}_3)(\mu_3:\eta^2:\eta^2:\eta^2\text{-C}_6\text{H}_6)]$ (**10**). The molecular structure of **10** is shown in Figure 2 with relevant structural parameters listed in Table I and Tables S2B and S3B (supplementary material).

The equatorial carbonyl ligands and phosphine phosphorus atom lie approximately in the plane of the metal triangle, with the Os–Os distances showing considerable variations (2.828 (1)–2.938 (1) Å). The planar C_6 ring adopts the μ_3 -face-capping mode (rms deviation from planarity = 0.007 Å), lying 2.17 Å above the plane defined by the three osmium atoms and the dihedral angle between these two planes is just 1.2°. There is no suggestion of marked double bond fixation in the μ_3 -benzene ligand, the “bonded” and “nonbonded” C–C distances averaging to 1.40 (2) and 1.43 (2) Å, respectively. Similarly, no significant variations among the Os–C_{carbonyl} lengths are observed, and the bond parameters for the PPh_3 ligand are normal.

Substitution by π -Alkene Ligands. η^2 -Alkene-triosmium complexes are not widely encountered since the π -bound alkenes are typically labile and/or susceptible to oxidative addition reactions.^{24a,26} η^2 -Ethylene,²⁷ fluoroalkene,²⁸ and chelating vinyl acetate²⁹ ligands have been previously crystallographically characterized in Os_3 systems, and in every case the olefin ligand occupies an equatorial coordination site and is approximately coplanar with the Os_3 triangle.

The MeCN ligand in **9** is easily substituted by simple olefins in high yielding reactions to afford η^2 -alkene complexes that retain the face-capping benzene ligand. Specifically, the olefin-triosmium complex $[\text{Os}_3(\text{CO})_8(\eta^2\text{-CH}_2\text{CH}_2)(\mu_3:\eta^2:\eta^2:\eta^2\text{-C}_6\text{H}_6)]$ (**11**) has been characterized through ¹H and ¹³C NMR studies³⁰ and by a single-crystal X-ray analysis.³¹

The molecular structure of **11** is shown in Figure 3 with structural parameters given in Table I and Tables S2C and S3C (supplementary material). The structure is derived from that of **1** with an equatorial carbonyl ligand on one metal atom being replaced by a π -bound ethylene ligand. The C_6 ring is strictly planar and lies parallel to the metal triangle (tilt angle 0.8°) at a distance of 2.17 Å above the plane. Although the high estimated standard deviations associated with the C–C distances preclude an accurate assessment of the bonding within the ring, there is again a suggestion of weak Kekulé-type distortion of the benzene ligand. Mean coordinated and noncoordinated C–C bond lengths of 1.41 (3) and 1.46 (3) Å for **11** may be compared with the corresponding distances of 1.41 and 1.51 Å in the parent complex **1**. The ethylene group is symmetrically coordinated in **11** and is displaced slightly from the Os_3 plane toward the benzene ligand (deviations: C(7) = 0.18 Å, C(8) = 0.46 Å). The C(7)–C(8) vector is twisted by 14° with respect to the triosmium plane, minimizing unfavorable interactions between proximal ethylene and benzene protons.

It is interesting to compare the stabilities of ethylene complex **11** and the π -adduct of the parent dodecacarbonyl, viz. $[\text{Os}_3$ -

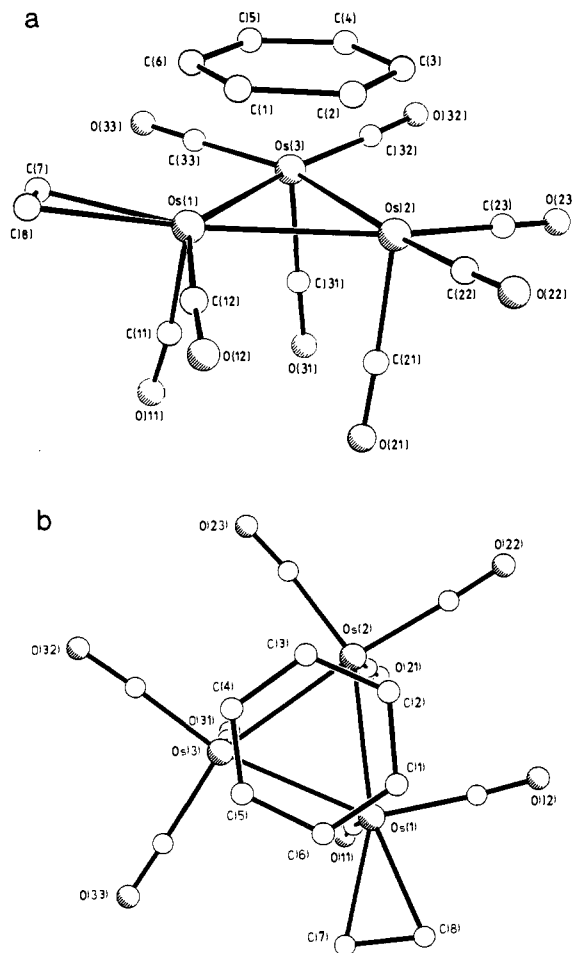


Figure 3. Molecular structure of $[\text{Os}_3(\text{CO})_8(\eta^2\text{-CH}_2\text{CH}_2)(\mu_3:\eta^2:\eta^2:\eta^2\text{-C}_6\text{H}_6)]$ (**11**).

$(\text{CO})_{11}(\eta^2\text{-CH}_2\text{CH}_2)]$ (**12**), prepared from the reaction of ethylene with **7**. Whereas CH_2Cl_2 solutions of **11** are not appreciably air-sensitive and are thermally stable to 50 °C, compound **12** is highly labile in the absence of external ethylene and is converted on thermolysis to the hydride vinylidene species $[(\mu\text{-H})_2\text{Os}_3\text{-}(\text{CO})_9(\mu\text{-CCH}_2)]$.³² It seems likely that the greater basicity of the $[\text{Os}_3(\text{CO})_8(\text{C}_6\text{H}_6)]$ fragment relative to the undecacarbonyl triosmium moiety accounts for this reactivity difference, with more extensive π -back donation to the olefin ligand in the former complex enhancing the stability of the metal–olefin interaction.

Bonding in Face-Capping Arene Complexes. Fenske–Hall Calculations for $[\text{Ru}_3(\text{CO})_9(\mu_3:\eta^2:\eta^2:\eta^2\text{-C}_6\text{H}_6)]$ (13**).** A fascinating structural feature of the μ_3 -arenes complexes discussed in this work is the apparent spectrum of multiple-bond localization seen in the face-capping ligands. Underlying electronic bases for these distortions have been probed via the Fenske–Hall quantum chemical technique by using $[\text{Ru}_3(\text{CO})_9(\mu_3:\eta^2:\eta^2:\eta^2\text{-C}_6\text{H}_6)]$ (**13**)³³ to model the osmium complex (**1**). Calculations were initially performed for **13** assuming C_{3v} symmetry and setting the long and short ring bond lengths to 1.51 and 1.41 Å, respectively, all other parameters being averaged, idealized data from the X-ray structure of **1**. A second calculation for the ruthenium cluster (**13a**) having all ring distances relaxed to an average value of 1.46 Å (but structurally unmodified otherwise) was undertaken, and the results were found to be comparable with those obtained above for **13**, i.e., the same orbital interactions are important in both cases. An orbital correlation diagram for **13** is shown in Figure 4.

(32) Johnson, B. F. G.; Lewis, J.; Pippard, D. A. *J. Chem. Soc., Dalton Trans.* 1981, 407.

(33) Preliminary experiments indicate that the triruthenium μ_3 -benzene complex **13** can be prepared following the synthetic strategy used for the preparation of the osmium analogue **1**.

(26) Deeming, A. J. In *Transition Metal Clusters*; Johnson, B. F. G., Ed.; Wiley: Chichester, 1981.

(27) Johnson, B. F. G.; Lewis, J.; Pippard, D.; Raithby, P. R. *J. Chem. Soc., Chem. Commun.* 1978, 551.

(28) (a) Dawoodi, Z.; Henrick, K.; Mays, M. J. *J. Chem. Soc., Chem. Commun.* 1982, 696. (b) Dawoodi, Z.; Mays, M. J.; Raithby, P. R.; Henrick, K. *J. Chem. Soc., Chem. Commun.* 1980, 641.

(29) Boyar, E.; Deeming, A. J.; Rothwell, I. P.; Henrick, K.; McPartlin, M. *J. Chem. Soc., Dalton Trans.* 1986, 1437.

(30) Gallop, M. A.; Johnson, B. F. G.; Keeler, J.; Lewis, J.; Heyes, S. J.; Dobson, C. M., following paper in this issue.

(31) Gallop, M. A.; Johnson, B. F. G.; Lewis, J.; Raithby, P. R. *J. Chem. Soc., Chem. Commun.* 1987, 1809.

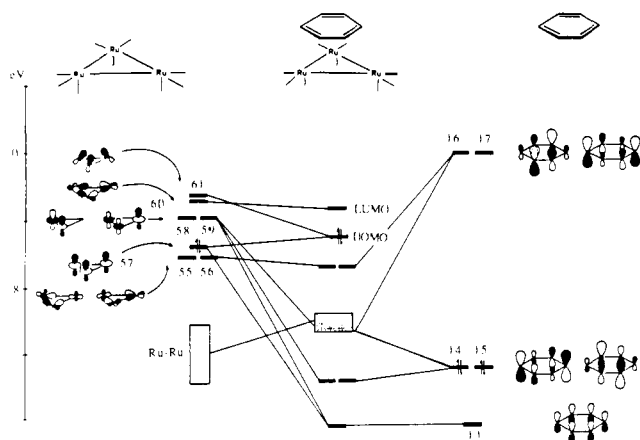


Figure 4. Correlation of the MOs of the $[\text{Ru}_3(\text{CO})_9]$ and $[\text{C}_6\text{H}_6]$ fragment to generate complex 13. The energies of the fragment orbitals are taken from the Fock matrix of the complex.

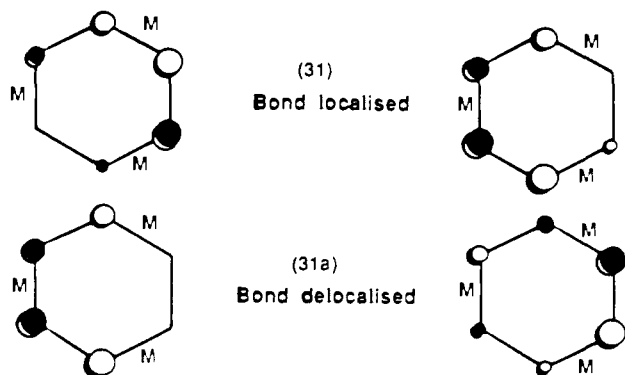


Figure 5. Benzene components of hybrid orbital e_{hy} from the two calculations for $[\text{Ru}_3(\text{CO})_9(\mu_3\eta^2\eta^2\eta^2\text{-C}_6\text{H}_6)]$ showing polarization of the π electron cloud.

The bonding in compound 13 is considered in terms of the interaction of the orbitals of its constituent fragments $\text{Ru}_3(\text{CO})_9$ and C_6H_6 . Hoffmann³⁴ has previously constructed the frontier orbitals of C_{3v} $\text{Fe}_3(\text{CO})_9$, and his scheme differs from ours only in the greater stabilization of orbital 61. The benzene π -MOs look slightly unfamiliar because of the reduction in symmetry caused by bond length alternation, though the general form is as for unperturbed C_6H_6 . The important bonding interactions are as expected on symmetry grounds. Overlap of the degenerate HOMO of the benzene ring with the vacant $2e$ acceptor orbitals, MOs 58 and 59, on the cluster fragment results in ring-to-metal π donation, while π -back bonding from the $[\text{Ru}_3(\text{CO})_9]$ fragment, MOs 55 and 56, is achieved via overlap with the benzene LUMO. Mulliken populations for the arene ring after complex formation show that the HOMO occupancy is reduced from 4 to 1.71 electrons. The LUMO, MOs 16 and 17, gains electrons. Cluster fragment orbitals 57 and 60 have little interaction with the ring orbitals and are carried through to become the HOMO and LUMO, respectively, of 13. The Mulliken π -overlap populations for the C-C bonds eclipsing the Ru atoms are greater than for the noneclipsing bonds (0.575 vs 0.489e) consistent with the bond alternation described. Significantly, the Mulliken π -overlap populations for the C-C bonds in 13a again alternate around the ring (0.549 and 0.518e; cf. uncomplexed, aromatic benzene 0.552e), suggesting that the bond length alternation found in the X-ray analysis has an internal, electronic basis and is not a consequence of intermolecular forces in the lattice. Contributions from σ orbitals to C-C overlap show little polarization in the face-capping ligand.

An explanation for the alternation of the C-C bond overlaps lies in the 3-fold symmetry of the $\text{Ru}_3(\text{CO})_9$ fragment. Under

C_{3v} symmetry the e_{1g} and e_{2u} benzene orbitals are both allowed to mix upon overlap of the benzene ring with a cluster fragment orbital of the same symmetry and appropriate energy. Such mixing is observed in the complex MOs 62 and 63, with these MOs containing approximately 11% benzene character (8% benzene LUMO and 3% HOMO in 13). The effect of mixing the HOMO and LUMO of the benzene in an occupied MO of complex 13 is to direct electron density out of the noneclipsing C-C bonds and into the bonds spanning the ruthenium atoms. The perturbed ring orbitals in 13 and 13a are represented in Figure 5, which illustrates in-phase overlap across the Ru atoms and out-of-phase overlap in the alternate bonds.

Kekulé-type distortion should be maximized when the hybrid orbital(s) contain equal and substantial contributions from benzene orbitals 14 through 17. There should exist, then, an optimum energy window for the frontier orbitals of the metal triangle within which a substantial localization of the π -electron cloud is induced. This suggests a rationalization for the structural trends noted in this study, since replacement of CO by weaker π -acids (PPh_3 or C_2H_4) or substitution of $\text{M}(\text{CO})_3$ by the more electron-rich $\text{M}'\text{Cp}$ residue would lead to changes in the effective electronegativity and orbital topologies of the trimetal fragment.

Mixing between the highest occupied and lowest unoccupied benzene π -orbitals is thought to be the cause of the small (but significant) bond length alternation (0.017 (2) Å) found in the neutron diffraction study of $[\text{Cr}(\eta^6\text{-C}_6\text{H}_6)(\text{CO})_3]$ by Rees and Coppens.³⁵ Here the common interaction is with hybrid orbitals formed by coupling of (mainly) metal $d_{x^2-y^2}$ and d_{xy} with the carbonyl 2π acceptor orbitals, decreasing C-C π -overlap along the ring edges eclipsing Cr-CO bonds and increasing overlap populations for the staggered C-C bond set.³⁶ Coupling of the benzene HOMO and LUMO is forbidden under D_{6h} symmetry, and structural studies on $[\text{Cr}(\eta^6\text{-C}_6\text{H}_6)_2]$ show no evidence for bond fixation in either ring.³⁷

There is a second important arene orbital mixing interaction associated with distortion of the face-capping ligand that leads to net ring expansion. Allowing the C-H bonds to bend out-of-plane away from the metal triangle mixes into the π^* LUMO a higher lying C-C σ antibonding level to give an acceptor hybrid that is both lower in energy and better suited for overlap with the metal-based donor orbitals.³⁸ Our calculations predict enhanced stabilization of complex 13 for a bending of 10–20°, in accord with the experimental data for clusters 2 and 5 above.

Benzene chemisorption at 3-fold sites on Rh, Ni, Pt, and Ag (111) crystal faces has been studied within the framework of extended Hückel theory, using "naked" cluster models for the metal surfaces.³⁹ C-H bond back-bending of $\sim 20^\circ$ is predicted on the Rh and Pt "surfaces" and is again attributed to rehybridization of the π system to maximize overlap with the metal orbitals. For the Rh substrates, simultaneous elongation of the six C-C bonds is found to be competitive with Kekulé distortion of the ring (distances alternate between 1.50 and 1.64 Å).^{39a} Internal mixing in the benzene π system is pinpointed as a contributory factor in this deformation, though greater importance is attached to distortions related to optimization of the Rh-C overlap. It is the admixture of CO π^* character into the valence orbitals of the metal fragment in 13/13a that permits an enhanced benzene $2e$ contribution to the hybrid wave function e_{hy} in the carbonyl cluster system (note that the frontier orbitals of the bare metal clusters are far removed in energy from the benzene LUMO and the latter contributes little to bonding). Although changes in metal size or other geometric effects could significantly influence bond localization in face-capping ligands (especially between first-

(35) Rees, B.; Coppens, P. *Acta Crystallogr.* 1973, B29, 2516.

(36) (a) Chinn, J. W., Jr.; Hall, M. B. *J. Am. Chem. Soc.* 1983, 105, 4930. (b) Byers, B. P.; Hall, M. B. *Organometallics* 1987, 6, 2319.

(37) (a) Haaland, A. *Acta Chem. Scand.* 1965, 19, 41. (b) Keulen, E.; Jellinek, F. *J. Organomet. Chem.* 1966, 5, 490.

(38) Albright, T. A.; Hoffmann, R.; Thibault, J. C.; Thorn, D. L. *J. Am. Chem. Soc.* 1979, 101, 3801.

(39) (a) Garfunkel, E. L.; Minot, C.; Gavezzotti, A.; Simonetta, M. *Surf. Sci.* 1986, 167, 177. (b) Anderson, A. B.; McDevitt, M. R.; Urbach, F. L. *Surf. Sci.* 1984, 146, 80.

(34) Schilling, B. E. R.; Hoffmann, R. *J. Am. Chem. Soc.* 1979, 101, 3456.

and second-row transition metals), relative orbital energetics account better for structural trends within the triosmium series 1, 10, and 11.

Face-Capping Benzene Complexes as Molecular Models for Benzene-Metal Surface Chemistry. Recent advances in the dynamical theory of low-energy electron diffraction (LEED) by ordered adsorbate overlayers have led to the structural characterization of several metal surface-benzene complexes by Somorjai and co-workers.¹³ On Rh(111), benzene coadsorbs with CO in two stoichiometries to give the surface complexes Rh(111)-(3 × 3)-C₆H₆ + 2CO (A) and Rh(111)-c[2(3)^{1/2} × 4]rect-C₆H₆ + CO (B), whose coordination geometries are accurately modeled by the carbonyl cluster compounds 1 and 2. In both overlayers benzene chemisorbs intact at 3-fold hcp-type sites and lies parallel to the close-packed surface, with an expanded C₆ ring showing in-plane Kekulé distortions. C-C bond distances alternate between 1.46 (15) and 1.58 (15) Å in (A) and between 1.31 (15) and 1.81 (15) Å in (B), the short bonds lying above single metal atoms while the long C-C bonds form bridges linking pairs of rhodiums. Metal-carbon bond distances also compare favorably between the surface and cluster complex regimes. In contrast, angle-resolved UV photoemission spectroscopic (ARUPS) studies on these Rh(111) systems provide no evidence for ring distortions, although trigonal deformations are detected by the same technique for benzene chemisorbed on Pt(111),⁴⁰ Ir(111),⁴¹ and Os(0001),⁴² surfaces. The degree of Kekulé distortion apparently increases from Pt through Os⁴⁰ and adsorption at 3-fold hollow sites is presumed. Theoretical studies of benzene chemisorption on Pt(111) and Rh(111) also predict maximum stability for surface complexes having C_{3v} site symmetry.³⁹

The recognition of structural analogies between metal cluster complexes and the adsorbed state has prompted the assertion that chemisorptive interactions may be described, to a first approximation, in terms of localized bonding between the adsorbate and neighboring surface atoms.¹⁴ Theoretical treatment based on cluster modeling of the adsorption site has shown that the largest portion of the chemisorptive enthalpy arises from "local" bonding contributions, although better estimates are obtained when non-nearest neighbor interactions are considered.⁴³ Our calculations on ruthenium complex 13 identify the same orbital interactions predicted for benzene chemisorption on close-packed Pt and Rh surfaces,³⁹ but we ascribe a substantially greater significance to metal-to-ligand π-back bonding (a large decrease in work function, Δφ = -1.52 eV, brought about by saturation coverage of C₆H₆ on Pt is consistent with net benzene-to-metal electron transfer in the surface regime).⁴⁴

Coadsorption of electropositive potassium with benzene on Pt(111) raises the metal s-d band in energy and, at high potassium coverage, promotes electron donation from the surface to the benzene LUMO.^{39,45} This suggests that cluster compound 13 (or 1 may be best regarded as a model for a cathodically charged surface complex or for benzene chemisorption on an earlier transition metal having a higher-lying Fermi level (e.g., at saturation coverage on W(100), Δφ = -0.3 eV, reflecting a dramatic reduction in benzene-to-metal π-donation relative to Pt).⁴⁶ Anodic charging of complex 1 may be simulated by protonation at the metal triangle to give [(μ-H)Os₃(CO)₉(μ₃:η²:η²:η²-C₆H₆)]⁺ (4), and it would be interesting to compare structural data for these two cluster compounds.

The decomposition chemistry of coordinated benzene is one further area in which formal analogies between the surface and cluster systems are evident. C-H bond scission constitutes an

important degradation pathway, and on atomically flat surfaces is particularly facile for earlier transition metals (e.g., C₆H₆ is completely dissociated at low coverage on W(100) at ambient temperature).⁴⁶ Broad-band visible irradiation of the triosmium cluster (1) results in efficient isomerization to the dimetalated benzyne complex [(μ-H)₂Os₃(CO)₉(μ₃:η¹:η²:η¹-C₆H₄)], offering a compelling model for the interconversion of associatively and dissociatively chemisorbed states of benzene via C-H activation.⁴⁷ On Rh(111), benzene decomposes thermally by decyclotrimerization to form three acetylenes that immediately fragment at the surface, affording chemisorbed methylidyne (CH) and ethynyl (C₂H) as the final products.⁴⁸ The strongly Kekulé-distorted Rh(111)-C₆H₆ + CO structure (B) may be viewed as a "snapshot" of this decyclization, and the establishment of a molecular cluster analogue for this C-C cleavage process remains an attractive synthetic goal.

Experimental Section

General Comments. Manipulations were performed under an atmosphere of purified nitrogen or argon using standard Schlenk techniques. Solvents were distilled from appropriate drying agents before use (CH₂Cl₂, hexane and octane, CaH₂; MeCN, P₂O₅; THF, Na/benzophenone). Me₃NO (Aldrich) was sublimed in vacuo prior to use. Cyclohexa-1,3-diene, trityl tetrafluoroborate, DBU, P(OMe)₃, PEt₃, PPh₃, CH₂CHPh, and CH₂CH^tBu were used as received from Aldrich. Ethylene, propene, vinyl fluoride, and buta-1,3-diene gases were used as supplied by Matheson. [(μ-H)₂Os₃(CO)₁₀] was prepared following the established literature procedure.⁴⁹ Thin-layer chromatographic separations were performed in air on 20 cm × 20 cm × 0.25 mm silica plates (Kieselgel 60 F₂₅₄) purchased from Merck.

IR spectra were recorded with a Perkin-Elmer 983 grating spectrophotometer using 0.1 mm path-length NaCl solution cells. NMR spectra were recorded on a Bruker AM400 (¹H, 400.13 MHz; ¹³C, 100.62 MHz) spectrometer. All ¹H and ¹³C shifts are reported positive if downfield from TMS and are referenced to the solvent resonance (CHDCl₂, ¹H, 5.32 ppm; CD₂Cl₂, ¹³C, 53.68 ppm). ³¹P shifts are reported relative to external P(OMe)₃. Mass spectra were recorded using an AEI MS12 instrument at 70 eV ionizing potential or on a Kratos MS 50 instrument in the positive ion fast atom bombardment (FAB) mode. Elemental analyses were performed by the University Chemical Laboratory microanalytical service.

[(μ-H)Os₃(CO)₉(μ₃:η²:η¹:η²-C₆H₇)] (3). [(μ-H)Os₃(CO)₉(μ₃:η²:η¹:η²-C₆H₇)] was prepared by the following modification of the literature procedure.¹⁵ Cyclohexa-1,3-diene (1.5 mL) was added to a solution of [(μ-H)₂Os₃(CO)₁₀] (350 mg) in *n*-octane (500 mL), and the mixture was heated under reflux at 125 °C for 50 min. The resulting yellow solution was evaporated under reduced pressure, and the residue was extracted with CH₂Cl₂ (30 mL). Filtration to remove any precipitated [Os₃(CO)₁₂] gave a solution of [(μ-H)Os₃(CO)₉(μ₃:η²:η¹:η²-C₆H₇)] that was typically converted directly to cationic [(μ-H)Os₃(CO)₉(μ₃:η²:η²:η²-C₆H₆)] [BF₄]⁻ by reaction with [Ph₃C][BF₄]. The pure cyclohexadienyl complex could be isolated as pale yellow crystals by thin-layer chromatographic separation of the crude material, eluting with CH₂Cl₂ (30%)/hexane (70%) and crystallizing from CH₂Cl₂/hexane: IR ν_{CO}/cm⁻¹ (CH₂Cl₂) 2086 (m), 2058 (s), 2030 (vs), 2007 (m), 1993 (m), 1942 (w); ¹H NMR δ (CDCl₃) 5.77 (t, *J* = 4.7 Hz, 1 H), 5.36 (ddt, *J* = 16.3 Hz, *J'* = 4.0 Hz, *J''* = 2.4 Hz, 1 H), 4.64 (dd, *J* = 8.4 Hz, 2 H), 2.82 (pdt, 2 H), 2.60 (dt, *J* = 2.1 Hz, 1 H), -19.35 (d, 1 H); MS, M⁺ = 908 (as required).

[(μ-H)Os₃(CO)₉(μ₃:η²:η²:η²-C₆H₆)] [BF₄]⁻ (4). [(μ-H)Os₃(CO)₉(μ₃:η²:η¹:η²-C₆H₇)] (300 mg) and [Ph₃C][BF₄]⁻ (600 mg) were heated in CH₂Cl₂ (15 mL) under reflux for 30 min. After cooling to room temperature, pale yellow microcrystals of the product were filtered and washed with CH₂Cl₂ (10 mL) and hexane (10 mL) (yield 310 mg, 95%): IR ν_{CO}/cm⁻¹ (MeNO₂) 2117 (m), 2092 (s), 2063 (vs), 2047 (m), 2031 (m), 1996 (w); ¹H NMR δ (acetone-*d*₆) 290 K 5.86 (s, 6 H), -21.50 (s, ¹*J*(¹⁸⁷Os-¹H) = 21 ± 1 Hz (from satellite spectrum, 1 H); 193 K 6.07 (m, 2 H), 5.89 (m, 2 H), 5.57 (m, 2 H), -21.48 (s, ¹*J*(¹⁸⁷Os-¹H) = 34 ± 1 Hz (from satellite spectrum), 1 H); ¹³C[¹H] NMR δ (acetone-*d*₆) 290 K 173.0 (br s, 4CO), 167.8 (br s, 2CO), 162.2 (br s, 2CO), ring carbons

(40) Somers, J.; Bridge, M. E.; Lloyd, D. R.; McCabe, T. *Surf. Sci.* **1987**, *181*, L167.

(41) Mack, J. U.; Bertl, E.; Netzer, F. P. *Surf. Sci.* **1985**, *159*, 265.

(42) Netzer, F. P.; Graen, H. H.; Kuhlbeck, H.; Neumann, M. *Chem. Phys. Lett.* **1987**, *133*, 49.

(43) Messmer, R. P. In *The Nature of the Surface Chemical Bond*; Rhodin, T. N., Ertl, G., Eds.; North Holland: Amsterdam, 1979.

(44) Abon, M.; Bertolini, J. C.; Billy, J.; Massardier, J.; Tardy, B. *Surf. Sci.* **1985**, *162*, 395.

(45) Garfunkel, E. L.; Maj, J. J.; Frost, J. C.; Farias, M. H.; Somorjai, G. A. *J. Phys. Chem.* **1983**, *87*, 3629.

(46) Bhattacharya, A. K. *J. Chem. Soc., Faraday Trans. 1* **1980**, *76*, 126.

(47) Gallop, M. A.; Johnson, B. F. G.; Lewis, J.; McCamley, A.; Perutz, R. N. *J. Chem. Soc., Chem. Commun.* **1988**, 1071.

(48) Koel, B. E.; Crowell, J. E.; Bent, B. E.; Mate, C., M.; Somorjai, G. A. *J. Phys. Chem.* **1986**, *90*, 2949.

(49) Knox, S. A. R.; Koepke, J. W.; Andrews, M. A.; Kaesz, H. D. *J. Am. Chem. Soc.* **1975**, *97*, 3942.

not observed; 193 K 180.6 (br s, 1CO), 173.2 (s, 2CO), 171.6 (br s, 2CO), 168.0 (s, 2CO), 162.7 (s, 2CO), 67.5 (s, 2C), 54.8 (s, 2C), 44.2 (s, 2C).

$[\text{Os}_3(\text{CO})_9(\mu_3\text{-}\eta^2\text{-}\eta^2\text{-}\eta^2\text{-C}_6\text{H}_6)]$ (**1**). $[(\mu\text{-H})\text{Os}_3(\text{CO})_9(\mu_3\text{-}\eta^2\text{-}\eta^2\text{-}\eta^2\text{-C}_6\text{H}_6)]$ [BF_4] (300 mg) was suspended in CH_2Cl_2 (60 mL) was stirred with 1,8-diazabicyclo[5.4.0]undec-7-ene (50 μL , 1.05 mol equiv) for 20 min to give a clear yellow solution. Purification by thin-layer or column chromatography, eluting with CH_2Cl_2 (40%)/hexane (60%), and crystallizing from CH_2Cl_2 /hexane gave lemon-yellow crystals of $[\text{Os}_3(\text{CO})_9(\mu_3\text{-}\eta^2\text{-}\eta^2\text{-}\eta^2\text{-C}_6\text{H}_6)]$ (yield 215 mg, 80%): IR $\nu_{\text{CO}}/\text{cm}^{-1}$ (CH_2Cl_2) 2076 (m), 2030 (vs), 1999 (m), 1978 (m), 1951 (sh); ^1H NMR (CD_2Cl_2) 4.42 (s, 6C); $^{13}\text{C}\{^1\text{H}\}$ NMR δ (CD_2Cl_2) 175.86 (s, 6CO), 175.82 (s, 3CO), 38.15 (s, 6C); MS, $M^{++} = 906$ (as required). Anal. Found (Calcd) for $\text{C}_{15}\text{H}_6\text{O}_9\text{Os}_3$: C, 20.16 (20.00); H, 0.80 (0.67).

$[\text{Os}_3(\text{CO})_8(\text{NCMe})(\mu_3\text{-}\eta^2\text{-}\eta^2\text{-}\eta^2\text{-C}_6\text{H}_6)]$ (**9**). $[\text{Os}_3(\text{CO})_9(\mu_3\text{-}\eta^2\text{-}\eta^2\text{-}\eta^2\text{-C}_6\text{H}_6)]$ (50 mg) was dissolved in CH_2Cl_2 (5 mL), and the solution was cooled to ca. 0 °C. A solution of Me_3NO (4.15 mg, 1.05 mol equiv) in MeCN (2 mL) was added dropwise, and the mixture was stirred for 15 min at room temperature. The reaction was monitored by IR spectroscopy, ensuring complete conversion of the starting material. Solvent was removed in vacuo, and the crude product was used directly. Analytically pure material could be obtained by TLC separation of the residue, eluting with MeCN (10%)/ CH_2Cl_2 (30%)/hexane (60%). Extraction of the bright yellow band with MeCN and evaporation in vacuo afforded deep yellow microcrystals of $[\text{Os}_3(\text{CO})_8(\text{NCMe})(\mu_3\text{-}\eta^2\text{-}\eta^2\text{-}\eta^2\text{-C}_6\text{H}_6)]$ (yield 43 mg, 85%): IR ν_{CO} (MeCN) 2054 (s), 2012 (vs), 1985 (vs), 1971 (sh), 1912 (w); ^1H NMR δ ($\text{CD}_2\text{Cl}_2/\text{CD}_3\text{CN}$, 10:1) 295 K 4.34 (br s, 6 H), resonance for coordinated MeCN not observed; 195 K major isomer 4.4 (v br s, 6 H), 2.33 (s, 3 H); minor isomer 4.06 (br s, 2 H), 3.94 (br s, 2 H), 3.68 (br s, 2 H), 2.80 (s, 3 H); isomer ratio ~ 5:1 MS, M^{++} (919) not observed. Anal. Found (Calcd) for $\text{C}_{16}\text{H}_9\text{NO}_8\text{Os}_3$: C, 21.71 (21.03); H, 1.21 (0.98); N, 2.29 (1.53).

$[\text{Os}_3(\text{CO})_8(\text{PPh}_3)(\mu_3\text{-}\eta^2\text{-}\eta^2\text{-}\eta^2\text{-C}_6\text{H}_6)]$ (**10**). $[\text{Os}_3(\text{CO})_8(\text{NCMe})(\mu_3\text{-}\eta^2\text{-}\eta^2\text{-}\eta^2\text{-C}_6\text{H}_6)]$ (40 mg) and PPh_3 (14 mg, 1.2 mol equiv) were stirred in CH_2Cl_2 (10 mL) for 15 min at room temperature. Bright yellow microcrystals of the product were obtained by TLC separation of the reaction mixture, eluting with CH_2Cl_2 (50%)/hexane (50%), and crystallization from CH_2Cl_2 /hexane (yield 46 mg, 93%): IR $\nu_{\text{CO}}/\text{cm}^{-1}$ (CH_2Cl_2) 2057 (s), 2018 (vs), 1991 (s), 1975 (m), 1962 (sh), 1943 (w), 1920 (w); ^1H NMR δ (CD_2Cl_2) 7.30–7.45 (m, 15 H), 3.87 (d, $J_{\text{PH}} = 1.8$ Hz, 6 H); $^{13}\text{C}\{^1\text{H}\}$ NMR δ (CD_2Cl_2) 183.96 (d, $J_{\text{PC}} = 8.0$ Hz, 2CO), 177.39 (s, 6CO), 133.34 (d, $J_{\text{PC}} = 10.1$ Hz, 6C, ortho), 130.75 (d, $J_{\text{PC}} = 3.0$ Hz, 3C, para), 128.78 (d, $J_{\text{PC}} = 11.1$ Hz, 6C, meta), 36.56 (s, 6C, C_6H_6); ipso resonance not observed; MS, $M^{++} = 1140$ (FAB) as required. Anal. Found (Calcd) for $\text{C}_{32}\text{H}_{21}\text{O}_8\text{Os}_3\text{P}$: C, 35.60 (35.72); H, 1.89 (2.29); P, 2.33 (2.63).

$[\text{Os}_3(\text{CO})_8(\eta^2\text{-CH}_2\text{CH}_2)(\mu_3\text{-}\eta^2\text{-}\eta^2\text{-}\eta^2\text{-C}_6\text{H}_6)]$ (**11**). A Schlenk tube containing $[\text{Os}_3(\text{CO})_8(\text{NCMe})(\mu_3\text{-}\eta^2\text{-}\eta^2\text{-}\eta^2\text{-C}_6\text{H}_6)]$ (50 mg) was evacuated and then filled with ethylene gas (1 atm). CH_2Cl_2 (5 mL) was slowly added at room temperature to give a clear yellow solution which was stirred under ethylene for 15 min. TLC separation of the reaction mixture, eluting with CH_2Cl_2 (50%)/hexane (50%), gave one yellow band that afforded $[\text{Os}_3(\text{CO})_8(\eta^2\text{-CH}_2\text{CH}_2)(\mu_3\text{-}\eta^2\text{-}\eta^2\text{-}\eta^2\text{-C}_6\text{H}_6)]$ on crystallization from CH_2Cl_2 /hexane (yield 47 mg, 96%): IR $\nu_{\text{CO}}/\text{cm}^{-1}$ (CH_2Cl_2) 2066 (s), 2027 (vs), 2003 (s), 1991 (sh), 1971 (m), 1959 (m); ^1H NMR δ (CD_2Cl_2) 293 K 3.96 (br s, 6 H), 2.03 (br s, 4 H); $^{13}\text{C}\{^1\text{H}\}$ NMR δ (CD_2Cl_2) 292 K 180.37 (s, 2CO), 176.83 (s, 6CO), 43.42 (br s, 6C, C_6H_6), 27.62 (s, 2C); MS, $M^{++} = 906$ (as required). Anal. Found (Calcd) for $\text{C}_{16}\text{H}_{10}\text{O}_8\text{Os}_3$: C, 21.37 (21.33); H, 1.22 (1.11).

Crystallographic Analyses. Crystals of **1**, **10**, and **11** were grown by slow evaporation of solvent from CH_2Cl_2 /hexane solutions at -20 °C. The data collection crystals were mounted on thin glass fibers. Diffraction measurements were made on a Stoe STADI-4 automated diffractometer using Mo $K\alpha$ radiation. Unit cells were refined from 50 reflections in the range $20 < 2\theta < 25^\circ$ by using standard STADI-4 centering and least-squares routines. A profile fitting procedure was

applied to all intensity data to improve the precision of the measurement of weak reflections. Crystal data, data collection parameters, and results of the analyses are listed in Table I. All data processing was performed on the University of Cambridge IBM 3084Q mainframe computer. Absorption corrections of a Gaussian integration type were performed for each structure. Neutral atom scattering factors were obtained from standard sources, and anomalous dispersion corrections were applied.⁵⁰

The Os atoms in each structure were located by direct methods (SHELX76, EELS for **10** and **11** and SHELX86, TREF for **1** and the remaining non-hydrogen atoms from subsequent difference Fourier syntheses. For **1** the Os and O atoms were refined anisotropically, for **10** all non-hydrogen atoms except the phenyl carbons were refined anisotropically, the latter being fixed as rigid groups with C–C 1.395 Å, while for **11** all non-hydrogen atoms were refined anisotropically. For **10** hydrogen atoms were placed in idealized positions on the phenyl and benzene carbon atoms (C–H 1.08 Å) and allowed to ride on these atoms. The phenyl and benzene hydrogens were each assigned a common isotropic thermal parameter which was refined. Structures **1** and **11** were refined to convergence using full-matrix least squares and structure **10** by blocked full-matrix least squares. The final difference Fourier maps showed electron ripples close to the Os atom positions but no other regions of significant electron density. The weighting schemes employed gave satisfactory agreement analyses.

Fenske–Hall Calculations. Fenske–Hall quantum chemical calculations⁵¹ were performed on $[\text{Ru}_3(\text{CO})_9(\mu_3\text{-}\eta^2\text{-}\eta^2\text{-}\eta^2\text{-C}_6\text{H}_6)]$ (**13**). Geometrical parameters were as follows. The molecule was idealized to C_{3v} symmetry. All carbonyl ligands were terminal; six were lying in the Ru_3 plane and three were lying perpendicular to it. All Ru–C–O groups were linear, with Ru–C = 1.90 Å and C–O = 1.13 Å. The $\text{C}_{\infty}\text{-Ru-C}_{\infty}$ bond angle was an average taken from the X-ray crystal structure of $[\text{Os}_3(\text{CO})_9(\mu_3\text{-}\eta^2\text{-}\eta^2\text{-}\eta^2\text{-C}_6\text{H}_6)]$ (**1**). The benzene ring was parallel to the Ru_3 triangle, and the hydrogen atoms were initially in the plane of the C_6 ring; all C–H bond lengths were 1.08 Å. An Ru–Ru bond length of 2.88 Å was employed, this being an average distance based upon the crystal structure of **1**.

Two calculations were performed on **13**. In the first calculation alternating values of 1.51 and 1.41 Å were used for the C–C bonds within the benzene ring, the short bonds lying over the Ru atoms (with Ru–C = 2.33 Å). The second calculation used equal C–C bond lengths of 1.46 Å (Ru–C = 2.34 Å).

Fenske–Hall calculations employed single- ζ Slater functions for the 1s and 2s functions of C and O. The exponents were obtained by curve fitting the double- ζ functions of Clementi⁵¹ while maintaining orthogonal functions; the double- ζ functions were used directly for the 2p orbitals. An exponent of 1.16 was used for hydrogen. The Ru functions,⁵² chosen for the +1 oxidation state, were augmented by 5s and 5p functions with exponents of 2.20.

Acknowledgment. We thank Dr. C. E. Anson for the vibrational spectroscopic measurements. M.A.G. gratefully acknowledges the Royal Commission for the Exhibition of 1851 and the University Grants Committee (New Zealand) for financial support. C.E.H. acknowledges the Royal Society for a 1983 Research Fellowship. S.M.O. thanks the S.E.R.C. for financial support.

Supplementary Material Available: Tables of atomic positional and thermal parameters and complete bond lengths and angles of **1**, **10**, and **11** (12 pages); listings of observed and calculated structure factors for **1**, **10**, and **11** (38 pages). Ordering information is given on any current masthead page.

(50) *International Tables for X-ray Crystallography*; Kynoch Press: Birmingham, England, 1975; Vol. IV.

(51) Hall, M. B.; Fenske, R. F. *Inorg. Chem.* **1972**, *11*, 768.

(52) Clementi, E. *J. Chem. Phys.* **1964**, *40*, 1944.